The charge distribution in the cytoplasmic loop of subunit C of the F1F0 ATPase is a determinant for YidC targeting

Kol, Stefan; Nouwen, Nico; Driessen, Arnold J. M.

Published in:
The Journal of Biological Chemistry

DOI:
10.1074/jbc.M709408200

Publication date:
2008

THE JOURNAL OF BIOLOGICAL CHEMISTRY VOL. 283, NO. 15, pp. 9871–9877, April 11, 2008

The Charge Distribution in the Cytoplasmic Loop of Subunit C of the F_1F_0 ATPase Is a Determinant for YidC Targeting*

Received for publication, November 15, 2007, and in revised form, January 22, 2008 Published, JBC Papers in Press, February 14, 2008, DOI 10.1074/jbc.M709408200

Stefan Kol, Nico Nouwen[1], and Arnold J. M. Driessen[2]

From the Department of Molecular Microbiology, Groningen Biomolecular Sciences and Biotechnology Institute and the Zernike Institute of Advanced Materials, University of Groningen, 9751 NN Haren, The Netherlands

YidC is a member of the Oxa1 family of proteins that facilitates the membrane insertion of a subset of inner membrane proteins in *Escherichia coli*. YidC acts as an insertase for membrane insertion of subunit c of the F_1F_0 ATP synthase (F_0c), but the requirements for substrate recognition have remained unclear. Here, we have analyzed the role of the charged aminoacyl residues in F_0c in YidC targeting and membrane insertion. Binding experiments demonstrate that F_0c is targeted directly to YidC without the presence of a stable lipid surface-bound intermediate. Positive charges in the cytoplasmic loop of F_0c are important determinants for YidC binding and subsequent membrane insertion. These data support a model in which F_0c binds directly to YidC prior to its membrane insertion.

The *Escherichia coli* inner membrane protein, YidC, is a member of the cytochrome oxidase biogenesis (Oxa) membrane protein family, which functions in promoting membrane insertion in chloroplasts, mitochondria, and bacteria (1). YidC is an essential protein in *E. coli* and other bacteria. A fraction of the YidC is associated with the Sec-translocase, where it interacts with transmembrane segments (TMSs)[3] of nascent inner membrane proteins (IMPs) during membrane integration (2). In addition, YidC also functions as an independent entity in the insertion of IMPs. The major coat proteins of bacteriophage M13 and Pf3, which were initially thought to insert spontaneously (3), were the first identified substrates of this pathway (4, 5). The first authentic *E. coli* YidC substrate described was subunit c of the F_1F_0 ATP synthase (F_0c) (6), whereas recently, the mechanosensitive channel of large conductance, MscL, was proposed to be another substrate of the YidC pathway (7).

The YidC dependence of F_0c is of particular interest as it concerns a critical step in the assembly of the F_1F_0 ATPase. F_0c is a component of the membrane-embedded F_0 sector that associates with the cytosolic F_1 domain ($\alpha_3\beta_3\gamma\delta\epsilon$) to assemble into a functional F_1F_0 ATPase. In *E. coli*, multiple F_0c subunits assemble into a decameric ring structure (8), which interacts with two b subunits and one a subunit (F_0b and F_0a, respectively). The F_1F_0 ATPase plays a central role in the energy metabolism of the cell, converting the energy stored in a transmembrane electrochemical gradient of protons into the synthesis of ATP from ADP and inorganic phosphate. During the catalytic cycle, F_0c becomes protonated at an aspartic acid at position 61 in the second TMS. This residue is located at the subunit a/c interface, and protonation induces a rotation of the c-ring whereupon another F_0c can be protonated by F_0a. This process drives the rotation of subunit γ within the $\alpha_3\beta_3$ hexamer of F_1, and by conformational changes in the catalytic nucleotide binding sites, causes the synthesis and release of ATP (9, 10). The biogenesis of the F_1F_0 ATPase has been studied in some detail. The current model is that upon the YidC-mediated insertion, F_0c assembles into a decameric ring structure (6, 8, 12) that subsequently interacts with the F_0a/$(F_0b)_2$ subcomplex (13). It is commonly believed that, in the next stage, the preassembled F_1 sector binds to the membrane-embedded F_0 sector to form the functional ATPase. *In vitro*, mixing of the separately purified sectors results in the restoration of coupled ATPase activity (14).

The mechanism by which YidC inserts IMPs into the membrane is poorly understood. Analysis of the physicochemical properties of YidC-only substrates may provide further insights in this process. Although the currently identified substrate range of the YidC-only pathway is relatively small, a common feature of these membrane proteins is their small size, their hydrophobicity, and the presence of short hydrophilic periplasmic regions. M13 phage procoat protein (73 amino acids) and the *E. coli* MscL (136 amino acids) and F_0c (79 amino acids) are similar in structure and contain two TMSs (or a signal sequence and TMS). The *Pseudomonas aeruginosa* Pf3 major coat protein (44 amino acids) contains only one TMS. Although *in vivo* depletion of the bacterial SRP component Ffh interferes with membrane assembly of a tagged F_0c variant (15), reconstitution studies have demonstrated that M13, Pf3, and F_0c are all targeted to YidC in a SRP-independent manner (6, 16, 17). MscL, on the other hand, seems to utilize SRP (7). Currently, it is unclear how ribosome targeting by SRP is achieved as YidC lacks the C-terminal extension of the mitochondrial Oxa1p needed for ribosome binding (18, 19). Moreover, it is not evident how SRP can discriminate between the YidC and Sec-translocases, *i.e.* the assumed default pathway for SRP-targeted

* This work was supported by a grant from the Earth and Life Science Foundation (ALW), which is subsidized by the Netherlands Organization for Scientific Research (NWO), and by European Community Grant LSHG-CT-2004-504601 (E-Mep). The costs of publication of this article were defrayed in part by the payment of page charges. This article must therefore be hereby marked "*advertisement*" in accordance with 18 U.S.C. Section 1734 solely to indicate this fact.

[1] Present address: Laboratoire de Symbiosis Tropicales et Méditerranéennes, Campus International de Baillarguet TA A-82/J 34398 Montpellier cedex 5, France.

[2] To whom correspondence should be addressed. Tel.: 31-50-3632164; Fax: 31-50-3632154; E-mail: a.j.m.driessen@rug.nl.

[3] The abbreviations used are: TMS, transmembrane segment; AMdiS, 4-acetamido-4′-maleimidylstilbene-2,2′-disulfonic acid; F_0c, F_1F_0 ATP synthase subunit c; IMV, inner membrane vesicle; IMP, inner membrane protein; SRP, signal recognition particle; PMF, proton motive force; Tricine, *N*-[2-hydroxy-1,1-bis(hydroxymethyl)ethyl]glycine.

nascent IMPs (20). Therefore, a major unresolved question is how these IMPs are targeted and recognized by YidC. Obviously, the hydrophobic character of the TMSs is important for YidC recognition in line with observations that TMSs of substrate proteins can be cross-linked to YidC (2). In addition, it has been suggested that the charge distribution in these IMPs may be critical for membrane binding and may possibly allow the electrophoretic translocation of the periplasmic regions and/or the formation of the final membrane topology (21). Before YidC was identified as an essential component for insertion, M13 procoat was believed to insert into the membrane spontaneously. Earlier studies with model systems suggested that the positive charges at the N and C termini of M13 procoat are important for an electrostatic binding to the membrane surface (22, 23), whereas the negative charges in the connecting loop were proposed to be needed for the proton motive force (PMF)-dependent insertion, allowing the protein to adopt its final membrane topology (24). Interestingly, the negative charges appear not to be necessary for insertion *per se* (25). Although those studies demonstrated that M13 procoat has a strong tendency to interact electrostatically with the membrane surface, it is unknown whether a membrane surface-bound form represents an authentic intermediate in YidC-mediated targeting and insertion. In contrast, membrane insertion of F_0c occurs independently of the PMF, whereas its membrane topology is reverse of that of M13 procoat (6). With F_0c, the short N and C termini are translocated, whereas the loop that connects the two TMSs remains in the cytosol.

Here, we have determined the role of the charged aminoacyl residues in the N terminus and cytosolic loop region of F_0c in YidC targeting and membrane insertion using *in vitro* assays. Our data demonstrate that positive charges in the cytosolic loop region of F_0c are important determinants for YidC recognition, and consequently, also for subsequent YidC-mediated membrane insertion. The data further suggest that membrane insertion does not occur via a stable membrane surface-bound intermediate of F_0c, consistent with a model wherein newly synthesized F_0c is targeted directly to YidC.

EXPERIMENTAL PROCEDURES

Strains and Plasmids—E. coli strain A19 was used to obtain the S135 lysate (26). Strain SF100 (27) was used for topology determination and overexpression of YidC (28). Strain JS7131 (4), in which the *yidC* gene is under control of the *araBAD* promoter, was grown overnight in Luria-Bertani (LB) medium at 37 °C supplemented with 0.2% arabinose and 25 μg/ml spectinomycin. Cells were harvested, washed with warm LB, diluted to an OD_{660} of 0.4, and further grown in the presence of 0.2% glucose to deplete YidC or with 0.2% arabinose to generate non-depleted control cells. After every generation, the cultures were diluted with 1 volume of the same medium until the YidC-depleted cells stopped growing. Depletion was verified by immunoblotting with antibodies directed against YidC. All mutants were constructed in vector pET20AtpE-A79C (6) (see Table 1).

In Vitro Insertion, Binding, and Association Assays—The RiboMax transcription kit (Promega) was used for the synthesis of mRNA in a coupled transcription/translation system. Reactions were carried out for 20 min at 37 °C in the absence or in the presence of YidC-depleted or non-depleted inner membrane vesicles (IMVs) as described previously. A small sample of the reaction mixture was used as a synthesis control, and the remainder was treated with 0.4 mg/ml proteinase K for 30 min on ice in the presence or absence of 1% Triton X-100. Samples were trichloroacetic acid-precipitated and analyzed by 18% SDS-PAGE and phosphoimaging. Binding assays were performed in the same manner, but the remainder was loaded on top of a sucrose cushion consisting of 10 mM HEPES-KOH, pH 7.5, 100 mM KCl, 0.5 mg/ml bovine serum albumin, 20% sucrose (v/v) sucrose, 1 mM dithiothreitol and spun at 25 p.s.i. for 20 min. Pellets were resuspended in 50 mM HEPES-KOH, pH 7.5, trichloroacetic acid-precipitated and analyzed by 18% SDS-PAGE and phosphoimaging.

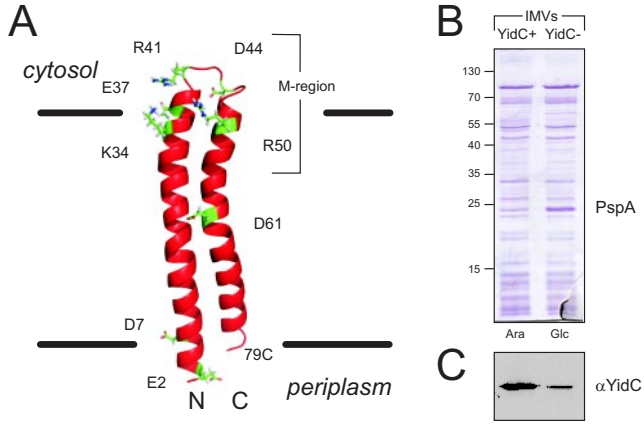

FIGURE 1. **Charge mutagenesis of F_0 subunit c and *in vivo* depletion of YidC.** *A*, position of charged residues in F_0c based on the structure of the rotor ring of the F-Type Na^+-ATPase from *Ilyobacter tartaricus* (1YCE.pdb (11)). This image was created with PyMOL. *N*, N terminus; *C*, C terminus. *B*, *in vivo* depletion of YidC induces the phage shock protein A (*PspA*) stress response. IMVs were prepared from strain JS7131 grown on arabinose ($YidC^+$ IMV) and glucose ($YidC^-$ IMV). *C*, YidC levels were determined by immunoblotting with anti-(α)YidC-IgG.

Labeling of F_0c A79C—To determine the topology of membrane-inserted wild-type F_0c and F_0c N++M−−−−−, *in vitro* labeling reactions were carried out in the presence of IMVs prepared from strain SF100. A small part of the reaction was removed as a synthesis control. The IMVs were subsequently reisolated by centrifugation through a sucrose cushion consisting of 10 mM HEPES-KOH, pH 7.5, 100 mM KCl, 0.5 mg/ml bovine serum albumin, and 20% (v/v) sucrose and resuspended in 50 mM HEPES-KOH, pH 7.5, 20% (v/v) glycerol. The membranes were then incubated for 20 min on ice with 0.15 mg/ml protease K. Digestion was stopped by the addition of 5 mg/ml phenylmethylsulfonyl fluoride. Labeling reactions were performed for 30 min at room temperature with 1 mM 4-acetamido-4′-maleimidylstilbene-2,2′-disulfonic acid (AMdiS) (Invitrogen) with and without Triton X-100 present. The labeling reaction was quenched with dithiothreitol, trichloroacetic acid-precipitated, and analyzed by Tricine-SDS-PAGE and phosphoimaging.

RESULTS

F_0 Subunit c Charge Mutagenesis—In the cytoplasmic membrane, F_0c forms a helical hairpin of two TMS. The short N and C termini are translocated into the periplasm, whereas the connecting loop region remains cytosolic (Fig. 1*A*). Except for the catalytic aspartic acid at position 61 in the

second TMS, charged aminoacyl residues are found only at the N terminus (Glu-2 and Asp-7) and in the cytosolic loop (Lys-34, Glu-37, Arg-41, Asp-44, and Arg-50) connecting the two TMSs (M-region). To investigate the contribution of these charges in the targeting of F_0c to YidC and the subsequent membrane insertion, we constructed a series of mutants in which the charge distribution and the net charge of the individual regions were systematically altered. To minimize changes in steric interactions with YidC, substitutions of amino acid residues were chosen such that they minimally affected the size of the side chain. To facilitate the determination of the membrane topology of the F_0c mutants, mutations were made in an F_0c derivative that contains a unique cysteine residue at position 79 and that, like wild-type F_0c, inserts into membranes in a YidC-dependent manner (6). The nomenclature used to describe the mutants first indicates the position in the protein, *i.e.* N or M, referring to the N terminus or the middle loop region, respectively, followed by the charges present in the region. For instance, the mutant that has the two N-terminal charges replaced by uncharged residues will be referred to as F_0c N00. Table 1 summarizes all the mutants used in this study.

Recognition of F_0c by YidC Is Dependent on the Charge Distribution in the M-region—To study the YidC dependence of F_0c binding and insertion, IMVs were isolated from *E. coli* strain JS7131 (4) grown in the presence of arabinose (wild-type cells, $YidC^+$ IMVs) or glucose (YidC-depleted cells, $YidC^-$ IMVs). Analysis of these IMVs by SDS-PAGE and immunoblotting showed that under YidC depleting conditions, the ~25-kDa phage shock protein A was induced (29) (Fig. 1*B*) and that the IMVs of cells grown in the presence of glucose contain only a very small amount of YidC (Fig. 1*C*). These IMVs were used in subsequent assays, unless indicated otherwise.

To determine the role of the charged aminoacyl residues in the M-region of F_0c in targeting to YidC, a combined binding/insertion assay was developed based on an *in vitro* transcriptional/translation reaction of F_0c in the presence of IMVs followed by isolation of the IMVs by centrifugation through a sucrose cushion. Since targeting, binding, and insertion are tightly coupled processes, the sedimentation assay monitors both the amount of membrane-associated F_0c and the amount of inserted F_0c. *In vitro* synthesized wild-type full-length F_0c co-sediments with $YidC^+$ IMVs (Fig. 2*A*, *lane 5*), whereas only low amounts associate with $YidC^-$ IMVs (*lane 6*). The latter levels are only slightly higher than the sedimentation in the absence of IMVs (*lane 4*). This suggests that the residual binding is due to the small residual amounts of YidC present in the $YidC^-$ IMVs. The efficiency of the *in vitro* synthesis of F_0c was not affected by the presence of IMVs (*lanes 1–3*). Increased levels of F_0c were found to co-sediment with IMVs containing overproduced levels of YidC (Fig. 2*E*). These data show that the sedimentation of F_0c with IMVs is strictly YidC-dependent and that newly synthesized F_0c has little tendency to associate with lipids or other membrane proteins present in the IMVs.

The sedimentation assay was further used to study the interaction of the remaining mutant F_0c proteins with YidC. Removal of only one of the positive charges in the M-region

TABLE 1
Site-directed F_0c mutants with altered charge distribution in the N terminus and the middle loop region

Wild-type F_0c	F_0c mutant[a]																		
	N00	N++	M+0+0+	M00000	M0−0−0	M0000+	M00+00	M+0000	M0−0−+	M+−0−0	M+−+−0	M+−0−+	M0−+−+	N++M−−−−−	M−−−−−
Glu-2 (GAA)	Gln (CAA)	Lys (AAA)												Lys (AAA)	
Asp-7 (GAT)	Asn (AAT)	Lys (AAA)												Lys (AAA)	
Lys-34 (AAA)				Leu (CTA)	Leu (CTA)	Leu (CTA)	Leu (CTA)		Leu (CTA)	Leu (CTA)			Leu (CTA)	Glu (GAA)	Glu (GAA)
Glu-37 (GAA)			Gln (CAA)	Gln (CAA)		Gln (CAA)	Gln (CAA)	Gln (CAA)							
Arg-41 (CGT)				Leu (CTT)	Leu (CTT)	Leu (CTT)		Leu (CTT)	Leu (CTT)		Leu (CTT)			Glu (GAA)	Glu (GAA)
Asp-44 (GAT)			Asn (AAT)	Asn (AAT)			Asn (AAT)	Asn (AAT)							
Arg-50 (CGT)				Leu (CTT)	Leu (CTT)		Leu (CTT)	Leu (CTT)		Leu (CTT)	Leu (CTT)	Leu (CTT)		Glu (GAG)	Glu (GAG)

[a] The indicated mutations were introduced into plasmid pET20AtpE-A79C. Only the changed residues with the corresponding substitutions are indicated. Codons are indicated between brackets. The nomenclature of the F_0c mutants is explained under "Results."

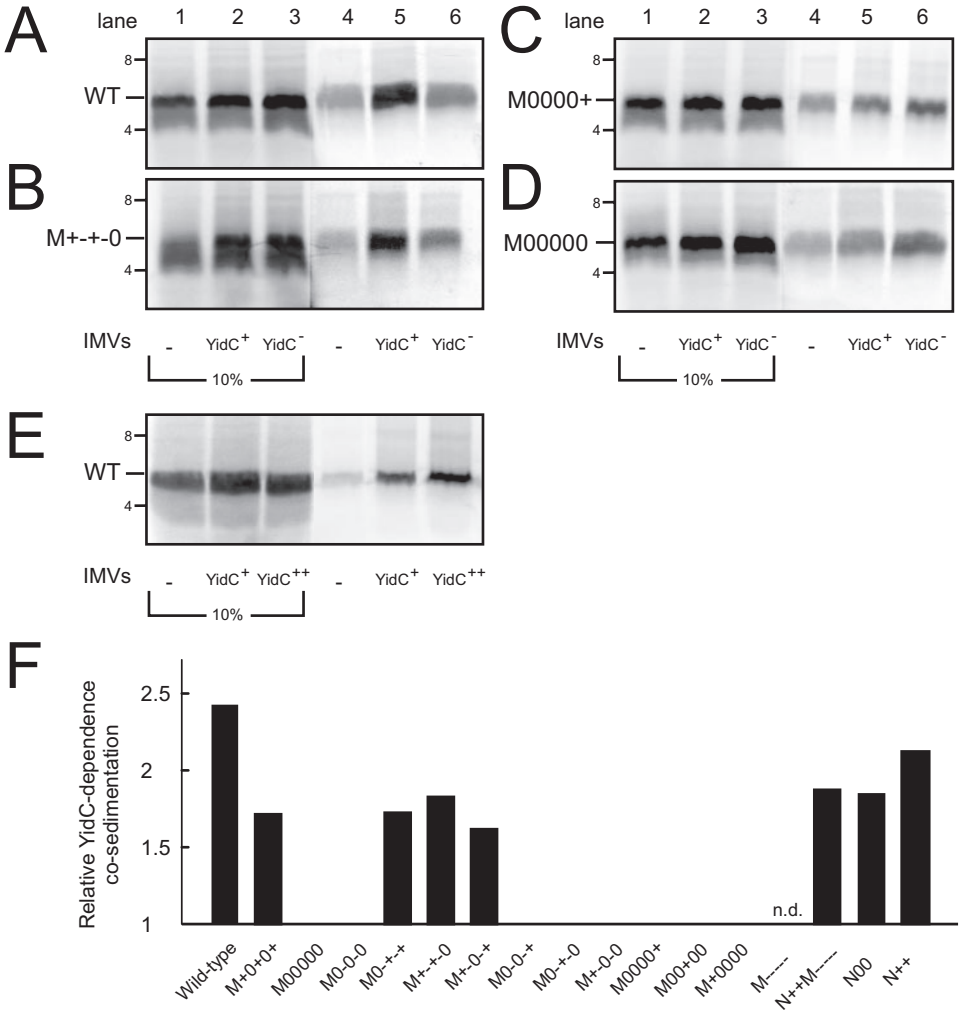

FIGURE 2. **Co-sedimentation of F_0c with YidC is strongly decreased upon removal of two or more positive charges in the M-region.** Wild-type (*WT*) F_0c (*A*), F_0c M+−+−0 (*B*), F_0c M0000+ (*C*), and F_0c M00000 (*D*) were synthesized in the absence of IMVs (*lanes 1* and *4*) or in the presence of 5 μg of YidC$^+$ IMVs (*lanes 2* and *5*) or YidC$^-$ IMVs (*lanes 3* and *6*). *E*, wild-type F_0c was synthesized in the absence of IMVs (*lanes 1* and *4*) or in the presence of 5 μg of SF100 IMVs (YidC$^+$, *lanes 2* and *5*) or YidC-overexpressed SF100 IMVs (YidC^{2+}, *lanes 3* and *6*). After translation, samples were directly analyzed on SDS-PAGE as translation controls (*lanes 1–3*) or spun through a sucrose gradient, and the collected membrane material was resuspended and trichloroacetic acid-precipitated (*lanes 4–6*). *F*, quantification of the co-sedimentation of charge mutants with YidC expressed as the ratio of F_0c bound to YidC$^+$ and YidC$^-$ IMVs. F_0c mutants defective in membrane association showed a ratio of 1 or less. *n.d.*, not determined.

(Fig. 2*B*, F_0c M+−+−0) had little effect on the amount of F_0c co-sedimented with the YidC$^+$ IMVs. On the other hand, when only a single positive charge (F_0c M0000+) (Fig. 2*C*) or no charge (F_0c M00000) (Fig. 2*D*) is present in the M-region, sedimentation is no longer YidC-dependent, and only very low levels of F_0c associate with the IMVs. Analysis of all M-region mutants in the YidC-dependent sedimentation assay (Fig. 2*F*) showed that the presence of two positive charges in the M-region suffices for efficient YidC-binding (F_0c M0−+−+, F_0c M+−0−+, and F_0c M+−+−0), whereas a further reduction to either one or no positive charge entirely abolishes the YidC-dependent sedimentation. Neutralization of the two negative charged amino acids in the M-region (F_0c M+0+0+) had little effect on the YidC-dependent sedimentation. With charge mutants of the N terminus of F_0c, sedimentation of F_0c N00 and F_0c N++ is somewhat reduced as compared with the wild-type (F_0c N−−) but remained YidC-dependent. Taken together, the above data indicate that the positively charged amino acids in the M-region of F_0c are important determinants for YidC recognition.

YidC-mediated Membrane Insertion of F_0c Is Dependent on the Presence of Positive Charges in the M-region—We next analyzed the set of mutants for membrane insertion using the previously described protease-protection assay. In the presence of YidC$^+$ IMVs, membrane-inserted wild-type F_0c becomes protease-resistant (6) (Fig. 3*A*, *lane 5*), whereas with YidC$^-$ IMVs, only a low level of protease-protected F_0c is observed (*lane 6*) that is slightly above the background levels observed in the absence of membranes (*lane 4*). Like wild-type F_0c, a substantial amount of protease-protected F_0c was observed when the two negatively charged aminoacyl residues at the N terminus were mutated (Fig. 3, *B* and *C*, *lane 5*; F_0c N00 and F_0c N++), although the YidC dependence of F_0c N00 was somewhat reduced. These data show that F_0c N00 and N++ insert into the membrane in a YidC-dependent manner and indicate that the charge distribution of the N terminus only marginally affects membrane insertion of F_0c.

Next, the membrane insertion of the M-region mutants of F_0c was analyzed (Fig. 3, *D–G*). Mutagenesis of only one of the three positively charged residues into a neutral or negatively charged aminoacyl residue hardly affected the YidC-dependent membrane insertion of F_0c (Fig. 3, *D* and *G*; F_0c M0−++−, M+−+−0, and M+−0−+). However, a marked decrease in the YidC-dependent membrane insertion was observed upon the mutagenesis of at least two positive charges (Fig. 3, *E* and *G*; F_0c M0−0−+, M0−+−0, and M+−0−0). Strikingly, the removal of all positive charges (Fig. 3*G*; F_0c M0−0−0), neutralization of the M-region (Fig. 3, *F* and *G*; F_0c M00000), or a complete replacement of the positively charged residues for glutamate (Fig. 3*G*, F_0c M−−−−−) completely abolishes the YidC-dependent membrane insertion. The latter mutant also excludes the possibility that the insertion defect is due to polarity effects of the introduced leucine residues. Neutralization of the two negatively charged amino acids (Fig. 3*G*; F_0c M+0+0+) barely affected the insertion. It should be noted that in particular with F_0c M00000, substantial levels of YidC-

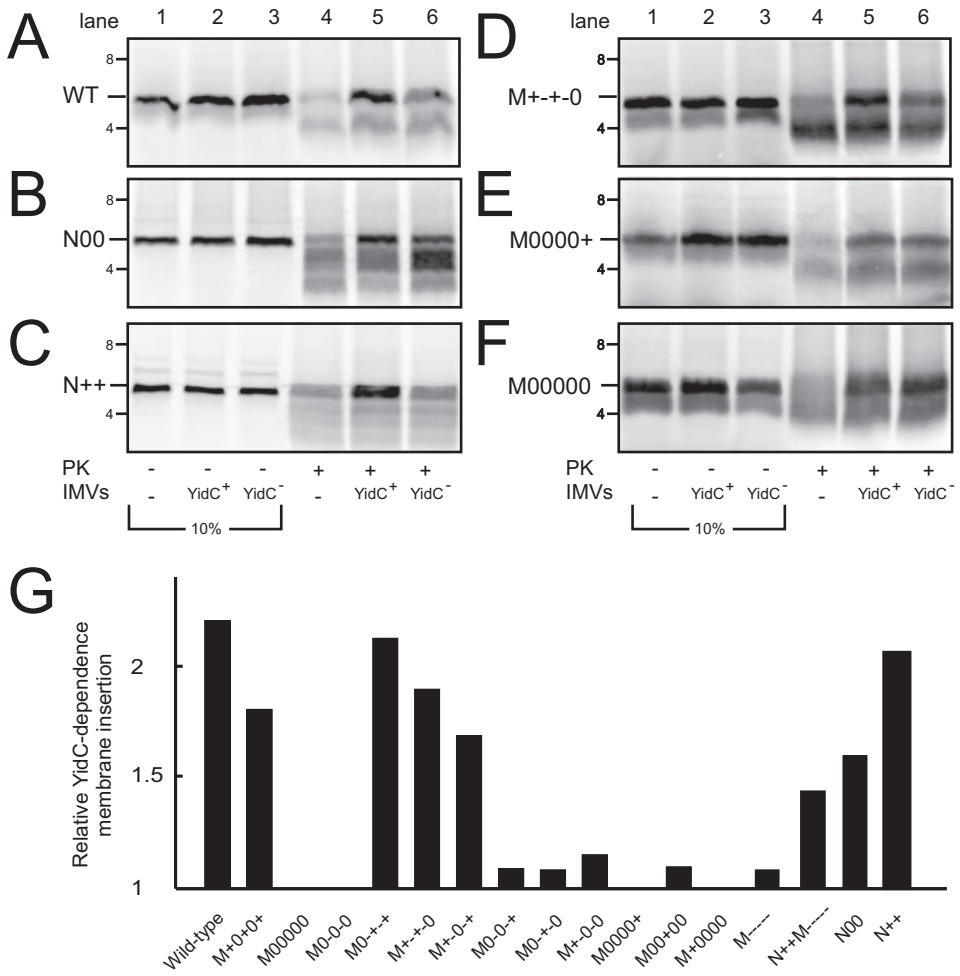

FIGURE 3. **Membrane insertion of F_0c is dependent on the presence of at least two positive charges in the M-region.** Wild-type (*WT*) F_0c (*A*), F_0c N00 (*B*), F_0c N++ (*C*), F_0c M+−−+−0 (*D*), F_0c M0000+ (*E*), and F_0c M00000 (*F*) were synthesized in the absence of IMVs (*lanes 1* and *4*) or in the presence of 5 μg of $YidC^+$ IMVs (*lanes 2* and *5*) or $YidC^-$ IMVs (*lanes 3* and *6*). After translation, samples were applied directly on SDS-PAGE as translation controls (*lanes 1–3*) or treated with 0.4 mg/ml proteinase K (*PK*) (*lanes 4–6*). *G*, quantification of the YidC dependence of membrane insertion of all charge mutants expressed as the ratio of F_0c insertion to $YidC^+$ and $YidC^-$ IMVs. F_0c mutants defective in membrane insertion showed a ratio of 1 or less.

but becomes accessible upon membrane solubilization with the detergent Triton X-100 (*lane 4*), as evidenced by a mobility change in SDS-PAGE due to the added mass of the AMdiS molecule. Incubation of membrane-inserted F_0c N++M−−−−− with AMdiS yields an altered labeling pattern as compared with wild-type F_0c with a larger fraction of the protease-protected full-length F_0c shifted toward the derivatized form (Fig. 4*D*, *lane 3*). This suggests that a major fraction of the F_0c N++M−−−−− has an altered topology as compared with the wild-type F_0c. Remarkably, in contrast to wild-type F_0c after proteinase K treatment of F_0c N++M−−−−−, a major protease-resistant fragment with a molecular size of ~5 kDa is observed, and only a little amount of full-length F_0c is observed (Fig. 4*A*, *lanes 5* and *6*; *asterisk*). As this protease-resistant fragment also increases in molecular size upon labeling with AMdiS (Fig. 4*D*, *lane 3* and *4*; *asterisk*), we conclude that it represents a C-terminal fragment of F_0c. The same fragment was observed when F_0c N++M−−−−− was synthesized *in vitro* with [^{35}S]cysteine instead of [^{35}S]methionine (data not shown). This suggests that F_0c N++M−−−−−inefficiently inserts in the membrane with a reversed topology and that this process is YidC-mediated.

independent membrane insertion are observed. The F_0c mutant with the reversed charge (F_0c N++M−−−−−) only weakly inserts into the membrane in a YidC-dependent manner (Figs. 3*G* and 4*A*). Overall, it is concluded that at least two positive charges in the M-region of F_0c are required for YidC-mediated membrane insertion. The exact position of these charges in the cytosolic loop region is of only minor importance.

A Reversed Charge Mutant of F_0c Shows Strong Membrane Binding but Poor Membrane Insertion—The charge balance of mutant F_0c N++M−−−−− is reminiscent of M13 procoat (3), a protein that has a membrane topology inverse of that of wild-type F_0c. As the F_0c N++M−−−−− also behaved differently in the binding and insertion assays as compared with wild-type F_0c, we decided to analyze its membrane topology. The F_0c derivatives used in this study contain a C-terminal cysteine residue (Cys-79) that in wild-type F_0c is translocated into the vesicle lumen. With the membrane-inserted wild-type F_0c, the cysteine residue is inaccessible for labeling with the membrane-impermeable reagent AMdiS (6) (Fig. 4*C*, *lane 3*)

DISCUSSION

Unlike the majority of the bacterial membrane proteins that co-translationally insert into the membrane in a SRP- and SecYEG-dependent manner, the F_0c protein (6), M13 procoat (4), and Pf3 (5) have all been shown to be solely dependent on YidC for membrane insertion. YidC functions as a membrane protein insertase (12, 21, 30), possibly forming an assembly and insertion scaffold in the membrane for small cytoplasmic membrane proteins. However, it is not known whether YidC-mediated membrane insertion involves a lipid surface-bound intermediate, nor is it clear how YidC recognizes its substrates. Here, we show that the positive charges in the cytosolic loop region (M-region) of F_0c are critical for YidC-mediated membrane insertion. Removal of these M-region charges affects the binding of F_0c to YidC and thus also results in a reduction of membrane insertion. At least two of the three positive charges must be present in this cytoplasmic loop of F_0c, but there is no strict requirement for the position of these residues

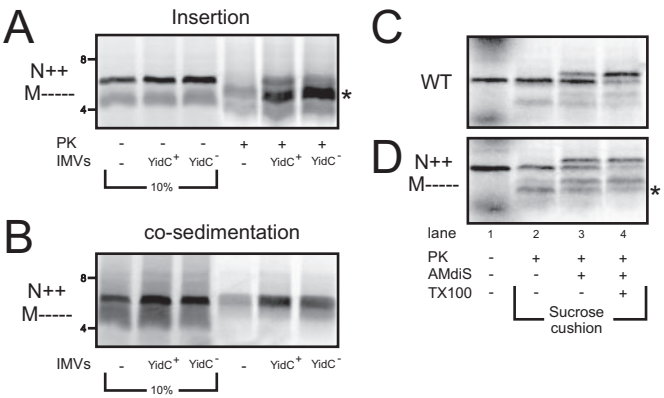

FIGURE 4. **Membrane insertion, co-sedimentation and topology analysis of F_0c N++M−−−−−.** *A*, reactions were carried out as described in the legend of Fig. 3. *PK*, proteinase K. *B*, reactions were carried out as described in the legend of Fig. 3, *A* and *B*. Wild-type (*WT*) F_0c (*C*) and F_0c N++M−−−−− (*D*) were synthesized in the presence of 5 μg of IMVs prepared from strain SF100. A small sample of the reaction was taken as a synthesis control (*lane 1*), and the remainder was spun through a sucrose cushion and treated with proteinase K. Digestion was stopped by the addition of phenylmethylsulfonyl fluoride, and the reaction was aliquoted and trichloroacetic acid precipitated (*lane 2*) or treated with AMdiS in the absence (*lane 3*) or presence of 1% (v/v) Triton X-100 (*TX100*) (*lane 4*). These samples were then trichloroacetic acid-precipitated and analyzed by Tricine-SDS-PAGE and phosphoimaging. When F_0c N++M−−−−− is treated with proteinase K, a proteolytic fragment is formed (*).

in the loop region. In analogy with the models proposed for membrane insertion of M13 procoat, we have previously suggested that the positive charges in the M-region might be important for an electrostatic interaction of F_0c with the membrane prior to its insertion (21). However, the co-sedimentation assay shows that binding of F_0c to IMVs is strongly dependent on the presence of YidC, with little or no F_0c associated with the lipid surface. Therefore, we conclude that YidC-mediated membrane insertion of newly synthesized F_0c does not occur via a stable membrane-bound intermediate but rather depends on a direct recognition of F_0c by YidC. The net charge of the M-region is only of minor importance, except that it should contain at least two positively charged aminoacyl residues. A similar mechanism of direct recognition by YidC may exist for M13 procoat, although earlier *in vitro* studies have shown that M13 procoat exhibits a high binding affinity and insertion activity with liposomes composed containing negatively charged phospholipids (23). Since the *in vivo* membrane insertion of M13 procoat strictly depends on YidC (Samuelson *et al.* 4), it is questionable whether such lipid-bound intermediate also exist in the physiological insertion pathway.

The arginine residue at position 41 in F_0c is required for the interaction with $F_1\epsilon$ and for coupling proton translocation through F_0 to ATP synthesis in F_1 (31). It is interesting to note that the two flanking positive charges are conserved in the c subunits of F-type Na^+- and H^+-ATPases, whereas no obvious interaction or catalytic function has been allocated to these residues. Possibly, their function is to assure a proper interaction with YidC or its homologues. The negatively charged amino acid residues at positions 37 and 44 are conserved in F_0c subunits, and the latter position can be cross-linked to $F_1\gamma$ (32). As these residues seem to be non-essential for YidC targeting and insertion, they likely play a structural role in the interaction with the F_1 sector.

Unlike the insertion of M13 procoat and Pf3, the membrane insertion of F_0c occurs independently of the PMF. Therefore, an electrophoretic effect of the transmembrane electrical potential ($\Delta\psi$) on the charged regions of F_0c, in particular on the N terminus, can be excluded. This region of F_0c needs to be translocated across the membrane and contains two amino acids with a negatively charged side chain, *i.e.* Glu-2 and Asp-7. On the other hand, unlike M13 procoat, the loop region of F_0c remains cytosolic and is not translocated. Our data suggest that the charge composition of the translocated N terminus of F_0c is not critical. Only the membrane insertion of F_0c N00 is somewhat disturbed and appears less YidC-dependent, whereas insertion of F_0c N++ occurs with similar efficiency and YidC dependence as wild-type F_0c.

Our *in vitro* data suggest that membrane insertion of the reversed charge mutant F_0c N++M−−−−− is highly inefficient (Fig. 4*A*). This charge distribution is reminiscent of M13 procoat that depends on the PMF for membrane insertion. The insertion defect of F_0c N++M−−−−− is, however, not due to an acquired requirement for the PMF as under the conditions tested, Yid^+ IMVs generate a PMF through the hydrolysis of ATP. F_0c N++M−−−−− still co-sediments with YidC IMVs (Fig. 4*B*), although the positively charged residues in the loop region have been removed. Possibly, the targeting involves the N-terminal positive charges in a manner that may resemble targeting of M13 procoat. In the absence of these positive charges, *i.e.* F_0c M−−−−− (Fig. 3*G*), membrane insertion is completely blocked, likely because of the complete loss of targeting. The cysteine accessibility study shows that a significant fraction of the membrane-associated and protease-resistant form of F_0c N++M−−−−− can be labeled by the membrane-impermeable alkylating agent AMdiS. This implies that the small amount of membrane-inserted F_0c either has adopted an inverted topology or represents an incomplete membrane-inserted state. In this respect, the prominent presence of a protease-resistant C-terminal F_0c fragment indeed suggests that only part of F_0c is shielded from protease digestion with the N terminus well accessible to the protease. Interestingly, albeit inefficiently, F_0c M00000 inserts independently from YidC (Fig. 3*G*), and only low levels of membrane association are observed (Fig. 2*D*).

We can now envisage a model of membrane targeting and insertion where F_0c first binds to YidC through an electrostatic interaction of the positively charged residues in the M-region and not via a membrane surface-bound intermediate. Subsequently, YidC acts as an insertase (12) and mediates the hydrophobic partitioning of the transmembrane segments of F_0c into the lipid bilayer with the concomitant helical hairpin formation. This model requires a direct physical interaction of F_0c with a cytoplasmic accessible and likely hydrophilic region in YidC. A suitable candidate for this interaction would be the first cytoplasmic loop, which contains an alternating stretch of positively and negatively charged residues. A previous deletion of this loop, however, did not seem to severely impair membrane insertion of a M13 procoat derivative (33), although it has been suggested that YidC exhibits different structural requirements for M13 and Pf3 (17). In these studies, F_0c was not tested. It would be of interest to map the sites of interaction of F_0c with

YidC, which will be the objective of future studies. Overall, the interaction between YidC and F_0c is likely governed by both hydrophobic and electrostatic forces. Substrate release and following insertion may therefore depend on a subtle balance between these forces.

Acknowledgments—We thank D. J. F. du Plessis, C. E. Price, J. de Keyzer, and J. G. de Wit for technical assistance and discussion.

REFERENCES

1. Luirink, J., von Heijne, G., Houben, E., and de Gier, J. W. (2005) *Annu. Rev. Microbiol.* 329–355
2. Scotti, P. A., Urbanus, M. L., Brunner, J., de Gier, J. W., von Heijne, G., van der Does, C., Driessen, A. J. M., Oudega, B., and Luirink, J. (2000) *EMBO J.* **19,** 542–549
3. Kuhn, A. (1995) *FEMS Microbiol. Rev.* **17,** 185–190
4. Samuelson, J. C., Chen, M., Jiang, F., Moller, I., Wiedmann, M., Kuhn, A., Phillips, G. J., and Dalbey, R. E. (2000) *Nature* **406,** 637–641
5. Chen, M., Samuelson, J. C., Jiang, F., Muller, M., Kuhn, A., and Dalbey, R. E. (2002) *J. Biol. Chem.* **277,** 7670–7675
6. van der Laan, M., Bechtluft, P., Kol, S., Nouwen, N., and Driessen, A. J. M. (2004) *J. Cell Biol.* **165,** 213–222
7. Facey, S. J., Neugebauer, S. A., Krauss, S., and Kuhn, A. (2007) *J. Mol. Biol.* **365,** 995–1004
8. Fillingame, R. H., Angevine, C. M., and Dmitriev, O. Y. (2002) *Biochim. Biophys. Acta* **1555,** 29–36
9. Capaldi, R. A., and Aggeler, R. (2002) *Trends Biochem. Sci.* **27,** 154–160
10. Weber, J., and Senior, A. E. (2003) *FEBS Lett.* **545,** 61–70
11. Meier, T., Polzer, P., Diederichs, K., Welte, W., and Dimroth, P. (2005) *Science* **308,** 659–662
12. Kol, S., Turrell, B. R., de Keyzer, J., van der Laan, M., Nouwen, N., and Driessen, A. J. M. (2006) *J. Biol. Chem.* **281,** 29762–29768
13. Stalz, W. D., Greie, J. C., Deckers-Hebestreit, G., and Altendorf, K. (2003) *J. Biol. Chem.* **278,** 27068–27071
14. Steffens, K., Schneider, E., Herkenhoff, B., Schmid, R., and Altendorf, K. (1984) *Eur. J. Biochem.* **138,** 617–622
15. van Bloois, E., Haan, G. J., de Gier, J. W., Oudega, B., and Luirink, J. (2004) *FEBS Lett.* **576,** 97–100
16. de Gier, J. W., Scotti, P. A., Saaf, A., Valent, Q. A., Kuhn, A., Luirink, J., and von Heijne, G. (1998) *Proc. Natl. Acad. Sci. U. S. A.* **95,** 14646–14651
17. Chen, M., Xie, K., Nouwen, N., Driessen, A. J. M., and Dalbey, R. E. (2003) *J. Biol. Chem.* **278,** 23295–23300
18. Jia, L., Dienhart, M., Schramp, M., McCauley, M., Hell, K., and Stuart, R. A. (2003) *EMBO J.* **22,** 6438–6447
19. Szyrach, G., Ott, M., Bonnefoy, N., Neupert, W., and Herrmann, J. M. (2003) *EMBO J.* **22,** 6448–6457
20. Valent, Q. A., Scotti, P. A., High, S., de Gier, J. W., von Heijne, G., Lentzen, G., Wintermeyer, W., Oudega, B., and Luirink, J. (1998) *EMBO J.* **17,** 2504–2512
21. van der Laan, M., Nouwen, N. P., and Driessen, A. J. M. (2005) *Curr. Opin. Microbiol.* **8,** 182–187
22. Kuhn, A., Wickner, W., and Kreil, G. (1986) *Nature* **322,** 335–339
23. Gallusser, A., and Kuhn, A. (1990) *EMBO J.* **9,** 2723–2729
24. Cao, G., Cheng, S., Whitley, P., von Heijne, G., Kuhn, A., and Dalbey, R. E. (1994) *J. Biol. Chem.* **269,** 26898–26903
25. Kuhn, A., Zhu, H. Y., and Dalbey, R. E. (1990) *EMBO J.* **9,** 2385–2389
26. Clark, A. J. (1963) *Genetics* **48,** 105–120
27. Baneyx, F., and Georgiou, G. (1990) *J. Bacteriol.* **172,** 491–494
28. van der Laan, M., Houben, E. N., Nouwen, N., Luirink, J., and Driessen, A. J. M. (2001) *EMBO Rep.* **2,** 519–523
29. van der Laan, M., Urbanus, M. L., ten Hagen-Jongman, C. M., Nouwen, N., Oudega, B., Harms, N., Driessen, A. J. M., and Luirink, J. (2003) *Proc. Natl. Acad. Sci. U. S. A.* **100,** 5801–5806
30. Serek, J., Bauer-Manz, G., Struhalla, G., van den Berg, L., Kiefer, D., Dalbey, R., and Kuhn, A. (2004) *EMBO J.* **23,** 294–301
31. Deckers-Hebestreit, G., and Altendorf, K. (1996) *Annu. Rev. Microbiol.* **50,** 791–824
32. Watts, S. D., Zhang, Y., Fillingame, R. H., and Capaldi, R. A. (1995) *FEBS Lett.* **368,** 235–238
33. Jiang, F., Chen, M., Yi, L., de Gier, J. W., Kuhn, A., and Dalbey, R. E. (2003) *J. Biol. Chem.* **278,** 48965–48972